ARL-TR-8836 ● Oct 2019

Density Functional Theory Study of the Impact of Impurities in Silicon Carbide Bulk and Grain Boundaries

by Cassidy Atkinson, Matthew Guziewski, and Shawn Coleman

NOTICES

Disclaimers

The findings in this report are not to be construed as an official Department of the Army position unless so designated by other authorized documents.

Citation of manufacturer's or trade names does not constitute an official endorsement or approval of the use thereof.

Destroy this report when it is no longer needed. Do not return it to the originator.

ARL-TR-8836 ● OCT 2019

Density Functional Theory Study of the Impact of Impurities in Silicon Carbide Bulk and Grain Boundaries

Cassidy Atkinson
Department of Materials Science and Engineering, University of Connecticut

Matthew Guziewski and Shawn Coleman
Weapons and Materials Research Directorate, CCDC Army Research Laboratory

REPORT DOCUMENTATION PAGE

Form Approved
OMB No. 0704-0188

1. REPORT DATE *(DD-MM-YYYY)*	2. REPORT TYPE	3. DATES COVERED (From - To)
October 2019	Technical Report	20 May–16 Aug 2019

4. TITLE AND SUBTITLE
Density Functional Theory Study of the Impact of Impurities in Silicon Carbide Bulk and Grain Boundaries

5a. CONTRACT NUMBER

5b. GRANT NUMBER

5c. PROGRAM ELEMENT NUMBER

6. AUTHOR(S)
Cassidy Atkinson, Matthew Guziewski, and Shawn Coleman

5d. PROJECT NUMBER
HIP-19-009

5e. TASK NUMBER

5f. WORK UNIT NUMBER

7. PERFORMING ORGANIZATION NAME(S) AND ADDRESS(ES)
CCDC Army Research Laboratory
ATTN: FCDD-RLW-ME
Aberdeen Proving Ground, MD 21005

8. PERFORMING ORGANIZATION REPORT NUMBER
ARL-TR-8836

9. SPONSORING/MONITORING AGENCY NAME(S) AND ADDRESS(ES)
DoD High Performance Computing (HPC) Modernization Program
US Army Engineer Research and Development Center
Vicksburg, MS 39180-6199

10. SPONSOR/MONITOR'S ACRONYM(S)
HPCMP

11. SPONSOR/MONITOR'S REPORT NUMBER(S)

12. DISTRIBUTION/AVAILABILITY STATEMENT
Approved for public release; distribution is unlimited.

13. SUPPLEMENTARY NOTES
ORCID IDs: Shawn Coleman, 0000-0002-5542-3161; Matthew Guziewski, 0000-0002-5761-720X

14. ABSTRACT

Density functional theory is used to determine the favorability of defects in the silicon carbide (SiC) system. Vacancy, substitutional, and interstitial defects are evaluated for bulk crystalline SiC and symmetric tilt ∑9 {122} SiC grain boundaries. Ten impurity atoms are considered; however, impurities of carbon, silicon, and silver are initially examined to compare calculated values to those in literature and to validate parameters used in calculations. All systems are relaxed, and the resulting energy difference is related to nondefected structures to determine the formation energy of the impurity. Lower formation energies determine more-stable, and likely more-favorable systems. Generally, carbon vacancies were found to be more stable than silicon vacancies, and substitutional defects were found to be more favorable than interstitial defects. The formation energy in both substitutional and interstitial sites increased as the atomic radius of the impurity atom increased. For grain boundaries, the calculations performed were more complicated and therefore took more computational hours to complete. For some of the elements, it was found that the grain boundary interstitial energies were lower than the most-favored defect site in the bulk lattice, which indicates a preferential desire to segregate at the interface. This project was performed with the intention of predicting structures that are likely to be encountered during processing SiC. This will allow probable cases to be further examined and classified as beneficial or hazardous to the mechanical properties of the material.

15. SUBJECT TERMS
modeling, simulations, interfaces, silicon carbide (SiC), density functional theory (DFT)

16. SECURITY CLASSIFICATION OF:			17. LIMITATION OF ABSTRACT	18. NUMBER OF PAGES	19a. NAME OF RESPONSIBLE PERSON
a. REPORT	b. ABSTRACT	c. THIS PAGE			Shawn Coleman
Unclassified	Unclassified	Unclassified	UU	24	19b. TELEPHONE NUMBER (Include area code) (410) 306-0697

Contents

List of Figures iv

List of Tables iv

Acknowledgments v

Preface: Impact of Summer Research Experience vi

1. Introduction 1

2. Materials and Methods 1

3. Results 5

4. Conclusions 10

5. References 11

Appendix. Example Scripts 12

List of Symbols, Abbreviations, and Acronyms 15

Distribution List 16

List of Figures

Fig. 1 Bulk SiC-3c: blue atoms are Si and red atoms are C 2

Fig. 2 Σ9 {122} SiC-3c symmetric tilt grain boundary 3

Fig. 3 Single atom defect structures modeled in bulk SiC-3c include a) atomic vacancy, b) substitution, and c) hexagonal interstitial defect. Yellow atoms represent inserted chemical species. 3

Fig. 4 Six interstitial sites chosen for analysis in the Σ9 {122} symmetric tilt grain boundary. Sites are labeled by their associated radii as calculated by Voronoi analysis. 4

Fig. 5 Bulk formation energy for 10 impurity atoms in two substitutional sites (Si and C) and three interstitial sites (tetrahedral Si, tetrahedral C, and hexagonal) 8

Fig. 6 Relative size of atomic radiuses of impurity atoms considered in this work 8

Fig. 7 Trends in formation energy for bulk SiC-3C substitutional and intestinal defects 9

Fig. 8 Most-favored interstitial formation energies for bulk and grain boundary calculations 9

List of Tables

Table 1 Chemical potential values for each impurity atom considered 5

Table 2 Cohesive energies calculated for the perfect system show good agreement between two different DFT codes 6

Table 3 Vacancy formation energies 6

Table 4 Substitutional and interstitial formation energies in bulk SiC-3C 6

Table 5 Calculated grain boundary calculations compared with reference 7

Table 6 Grain boundary energy (measured in angstroms) for interstitial sites found in the {122} symmetric tilt grain. Values marked with * are preliminary due to limited relaxation. 7

Acknowledgments

This research was sponsored by the High Performance Computing (HPC) Modernization Program and the HPC Internship Program. Cassidy Atkinson would like to thank College Qualified Leaders and the Army Educational Outreach Program for this opportunity, and Shawn Coleman and Matthew Guziewski for their assistance and mentorship.

Preface: Impact of Summer Research Experience

Background

I am a rising senior at the University of Connecticut majoring in Materials Science and Engineering. I aim to pursue a PhD after obtaining my undergraduate degree. In the past I have done research using density functional theory (DFT) to investigate chemical trends in aluminum alloy interfaces. I have also worked with the solidification and casting group in the University of Connecticut Foundry, where I have gained hands-on experience working with metals and metal processing. Most of my past research involved metals, so investigating ceramics was an adjustment. I was interested in an High-Performance Computing (HPC) internship at the US Army Combat Capabilities Development Command Army Research Laboratory because the project I would be working on was similar to research I have done in the past, but with the opportunity to have a much larger impact. I also was interested in an HPC internship to gain more experience working with high-performance computers and atomistic modeling.

Impact

I found the HPC Internship Program to be extremely informative and rewarding. With the work I did involving DFT in the past, I was provided with most of the models and the input files. Understanding how to choose appropriate parameters for the calculations I performed and what these various parameters meant was a skill I enjoyed developing. I now feel confident in starting Vienna Ab initio Simulation Package calculations from scratch and adjusting the parameters to enhance the efficiency. I also had no experience writing portable batch scripts. I now feel more comfortable with these. I had some experience with Python but am glad that I had the chance to practice using it more throughout the summer. I feel more confident after this internship experience that I would like to pursue a PhD. Talking to my mentors and other folks helped me realize that going to graduate school right after obtaining my bachelor's degree will be the best move for me. I also am appreciative of the various information on schools and fellowships that people I met provided me with. Overall, I am grateful for all the HPC Internship Program taught me, both about high performance computing—and about myself.

1. Introduction

Silicon carbide (SiC) is a commonly used ceramic in body armor, and is being further investigated as the binding matrix for future diamond–composite armor. While SiC has been studied significantly,[1] there has been limited work with regards to the energetics of the system after the introduction of impurities. Grain boundaries are of particular relevance, as they are known to influence fracture toughness,[2] and prior experiments have shown that impurity atoms have improved pure SiC performance by stabilizing intergranular films at grain boundaries.[3] Density functional theory (DFT) can aid in understanding how atomic-scale defects influence the thermodynamics of the system and help predict what structures are likely to form. This can help in targeting further mechanical response simulations. The goal of this project is to implement DFT to examine the impact of impurities within SiC by investigating both bulk and grain boundary structures. Note that this work considers impurities to be any atom inserted into the structure that does not match the motif of the pure basis set. These can include dopant atoms that are intentionally added to improve certain processing or performance metrics, atoms that are unintentionally introduced during processing that might alter performance metrics, and even self-interstitial atoms were atoms in the bulk are added to their ideal position. Investigating these impurities will help in the development of a more optimal microstructure within SiC by uncovering those impurities that do improve processing and performance metrics, with the eventual goal of creating improved armor for Soldiers in the field.

2. Materials and Methods

DFT is a computational modeling method that takes place on the atomic scale to analyze the electronic structure of a system. The results of DFT calculations can be used to predict optimal microstructure and mechanical behaviors of systems. There are many packages that can be used to perform DFT calculations. The package that was used for this project is the Vienna Ab initio Simulation Package (VASP).[4] The projector augmented wave method was used in the VASP calculations. This method uses pseudo-potentials and linear augmented-plane-wave methods to perform calculations as efficiently as possible.

There are many input and output files that can be implemented in VASP. The input files that were used for the performed calculations include the following: INCAR, which specifies the parameters the calculation should follow; KPOINTs, which are sampling points used to create a mesh for the calculation to perform over; POSCAR, which contains the initial positions of each atom in the simulation; and

POTCAR, which contains the pseudo-potential data for each element type used. The INCAR file can contain many different tags, most of which have default values associated with them. A portable batch system run script was also used to launch the calculations. On average, the calculations were submitted on 80 cores for 48 h. The number of nodes and time for the calculations were adjusted based on the complexity of the system. The output files that were mainly implemented in the calculations were the CONTCAR file, which contains the positions of each atom after the system has been relaxed, and the OUTCAR file, which contains detailed information about the VASP run. If a calculation did not complete when the submitted time ended, the CONTCAR file could be copied to the POSCAR file, and then the calculation could be restarted from where it left off. Examples of these scripts can be found in the Appendix.

Both bulk and grain boundary structures of SiC-3c were examined. The POSCAR files were created and could be seen in a visualization software such as OVITO[5] or VESTA.[6] Bulk systems, shown in Fig. 1, were examined first, and once they were verified by literature values, the Σ9 {122} symmetric tilt grain boundary was investigated. The Σ9 grain boundary, shown in Fig. 2, was chosen due to existing literature, allowing for the comparison of calculated values.[2] Bulk and grain boundary systems without defects were relaxed, and the energy from each was recorded before impurities were induced. Three types of defects were performed for each system: vacancy, substitutional, and interstitial defect structures. These defect structures are shown in Fig. 3.

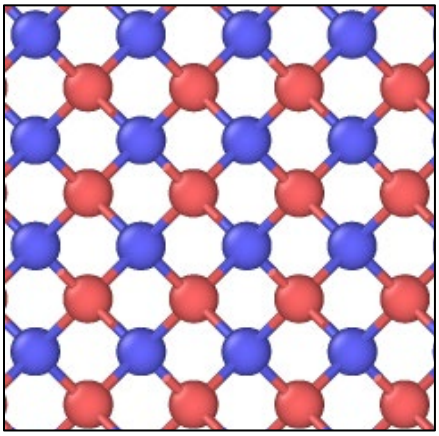

Fig. 1 Bulk SiC-3c: blue atoms are Si and red atoms are C

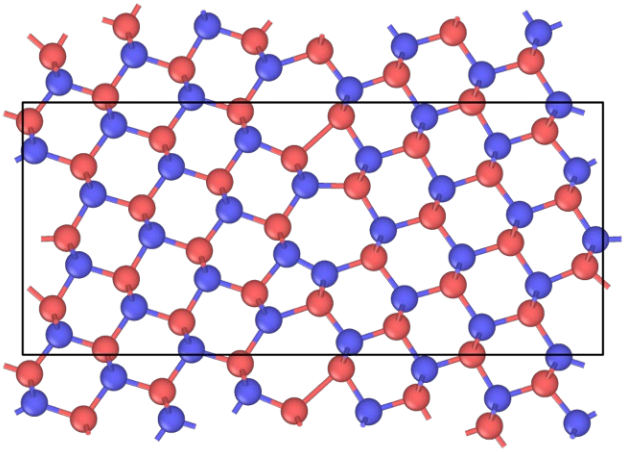

Fig. 2 Σ9 {122} SiC-3c symmetric tilt grain boundary

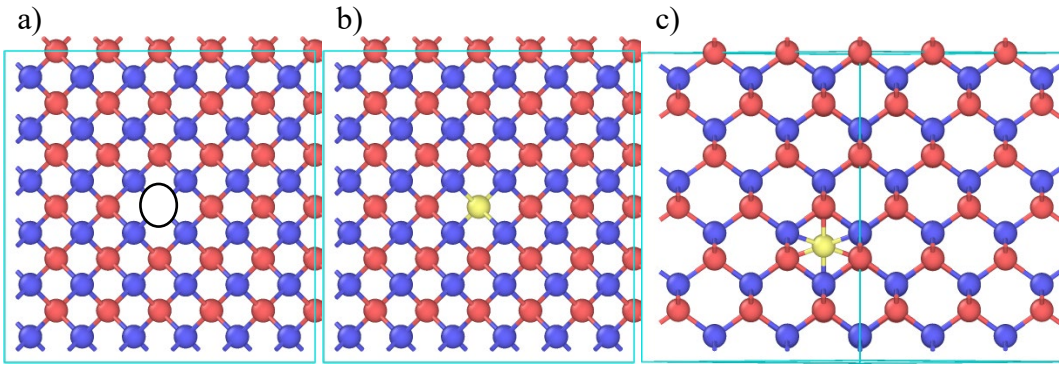

Fig. 3 Single atom defect structures modeled in bulk SiC-3c include a) atomic vacancy, b) substitution, and c) hexagonal interstitial defect. Yellow atoms represent inserted chemical species.

In the case of SiC, two types of vacancies can be formed, one where Si is removed and one where C is removed. Substitutional defects occur when an atom from the original structure is removed and replaced with an impurity atom. In line with vacancies, there are also Si and C respective substitutions. Interstitial defects are slightly more complicated than substitutional defects, and are formed by inserting an additional atom into the existing system. To do this, interstitial sites had to be found where it would be possible for this to take place. These sites were found using a Python script that uses Voronoi tessellation to identify free volume regions in the structure and then calculates their associated radius. For bulk structures, two different sizes of interstitial sites were found, corresponding to two types of interstitial defects. The two types were tetrahedral and hexagonal. Hexagonal sites have the impurity atom bonded to six neighbors, meaning that the impurity atom is bonded to both Si and C atoms. Tetrahedral impurities are bonded to four neighbors of only one type. Therefore, two different types result: Si-bonded and C-bonded. When the script was run for the Σ9 {122} symmetric tilt grain boundary, a multitude

of sizes and thus types of interstitial sites were found. Interstitial calculations within the grain boundary began by examining the six largest sizes in hopes of gaining an understanding of the different types of interstitial types and to minimize the number of calculations needed to be performed. The six sites chosen and their corresponding radii are shown in Fig. 4.

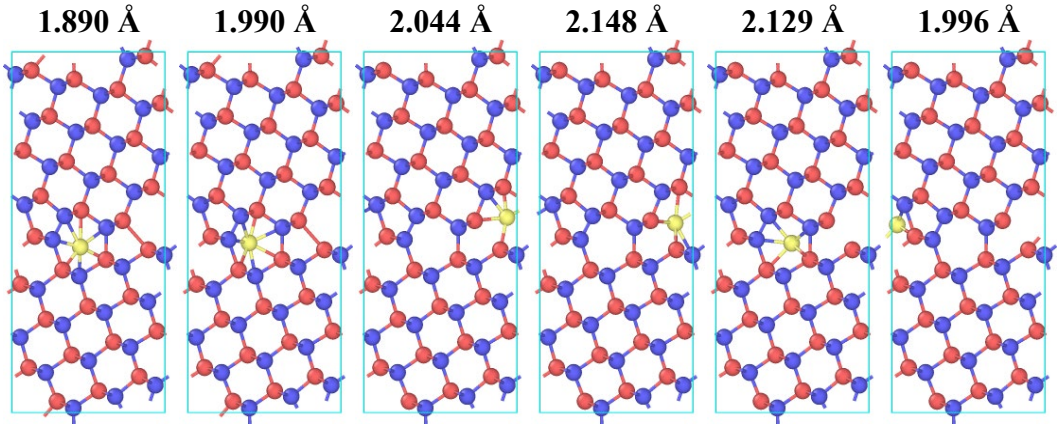

Fig. 4 Six interstitial sites chosen for analysis in the Σ9 {122} symmetric tilt grain boundary. Sites are labeled by their associated radii as calculated by Voronoi analysis.

Ten impurity chemical species were considered. Si and C were both considered impurities because the system is made of both. Silver (Ag), palladium (Pd), cesium (Cs), and tin (Sn) were examined because referenced literature examined these, and one goal was to be able to replicate the results. Oxygen (O) and nitrogen (N) were examined because they are common impurity atoms. Calcium (Ca) and sodium (Na) were recommended to be used as impurity atoms because they are commonly used processing aids.

The energy of bulk SiC and the Σ9 {122} symmetric tilt grain boundary was obtained without inducing defects in order to compare the values to literature as well as to use as reference values to determine the impact that defects had on the structures. For the bulk system, cohesive energy was calculated. This can be defined by

$$E_{cohesive} = \frac{E_{total}}{N}, \tag{1}$$

where E_{total} is defined as the energy simulated when the system is relaxed, and N is the number of particles. This method works for VASP because the energy resulting from individual Si and C atoms is already subtracted from the final energy the calculation displays. For grain boundaries, energy was calculated as follows:

$$E_{GB} = \frac{E_{total} - [N \cdot E_{SiC}]}{2A}, \tag{2}$$

where E_{total} is the simulation energy when the bicrystal grain boundary is relaxed, N is the number of SiC formula units, E_{SiC} is the energy per formula unit of SiC, and A is the area of the grain boundary.

To investigate the relative stability of the various atomic defects, formation energies were found for bulk and grain boundary systems. The formation energy for each structure was found using the following:

$$E_f = E_{defected} - E_{perfect} + \sum_I \Delta n_I \mu_I \,, \tag{3}$$

where $E_{defected}$ is the energy found when a defected system was relaxed, $E_{perfect}$ is the energy of a bulk system with no defects, Δn_I is the change in number of atoms of species I from the perfect cell to the defected cell, and μ_I is the chemical potential of species I. By accounting for the change in chemical composition, formation energies can be compared with varying number of atoms and different chemical elements.

3. Results

To calculate formation energies, chemical potentials were calculated for all the considered impurity atoms. These values were found by relaxing a structure of the ideal bulk (crystalline or gaseous) form of each impurity atom. The calculated values are found in Table 1.

Table 1 Chemical potential values for each impurity atom considered

Element	Chemical potential (eV)
Si	4.885
C	9.212
Ag	2.715
O	2.680
Pd	2.605
Sn	3.650
Cs	0.866
Ca	1.934
Na	1.312
N	4.540

Bulk SiC-3C calculations were performed first. To calculate the formation energy due to defects, the energy of a perfect crystal had to be known. This value was found by relaxing a system without defects. To verify the parameters used in the

VASP calculations, another DFT code called CASTEP[7] was run for comparison. The resulting cohesive energy values for both codes are found in Table 2.

Table 2 Cohesive energies calculated for the perfect system show good agreement between two different DFT codes

DFT code	Cohesive energy (eV)
VASP	–7.5311
CASTEP	–7.5241

When the cohesive energy value was used in the formation energy calculation, it was multiplied by the number of formula units of the system. Vacancy, substitutional, and interstitial calculations were performed next, and the results are found in Tables 3 and 4.

Table 3 Vacancy formation energies

Atom removed	Formation energy (eV)
Si	7.56
C	3.63

Table 4 Substitutional and interstitial formation energies in bulk SiC-3C

(eV)	Si	C	Ag	O	Pd	Sn	Cs	Ca	Na	N
Substitutional Si	…	3.01	6.08	2.78	2.10	2.21	12.09	5.46	6.69	1.78
Substitutional C	2.23	…	6.64	–4.13	1.20	6.55	11.43	9.33	8.49	–5.52
Tetrahedral Si	9.66	9.53	10.71	2.10	8.91	13.40	23.62	10.99	7.36	3.27
Tetrahedral C	7.90	10.40	9.72	5.65	7.09	13.40	23.73	10.32	6.83	6.03
Hexagonal	7.90	8.72	9.70	2.09	7.08	13.23	22.23	10.99	6.83	3.38

Grain boundary calculations were performed when bulk calculations were complete. The grain boundary energy of a nondefected grain boundary was calculated using VASP and compared with values obtained using CASTEP, as shown in Table 5.

Table 5 Calculated grain boundary calculations compared with reference

DFT code	Grain boundary energy (J/m^2)
VASP	1.369
CASTEP	1.346

These values were in good agreement, so it was deemed that the VASP parameters were acceptable to proceed with additional calculations. For the grain boundary simulations, only interstitial calculations were performed. The values for these calculations can be found in Table 6 for the six different sites identified by their associated Voronoi radii.

Table 6 Grain boundary energy (measured in angstroms) for interstitial sites found in the {122} symmetric tilt grain. Values marked with * are preliminary due to limited relaxation.

Energy	Si	C	Ag	O	Pd	Sn	Cs	Ca	Na	N
1.890 Å	9.79	8.83	10.59	–2.44	5.58*	14.09	18.45	9.92*	7.09	3.25
1.990 Å	11.13	9.20	11.13	–2.80	6.29	14.08	19.79	10.70*	7.88	2.69
2.044 Å	9.61	7.91	9.58	–5.10	4.65	14.37	17.28	9.77*	7.33	2.11
2.148 Å	6.11	9.35	10.01	–5.10	5.05	13.71	18.22	10.38*	7.86	3.21
2.129 Å	6.17	8.83	10.58	–0.21	5.51	14.08	18.45	9.48*	7.08	3.26
1.996 Å	9.60	9.03	9.57	–5.10	4.65	14.37	17.28	9.68*	7.32	3.22

Simulations to study other atomic defects within the Σ9 grain boundary are currently being developed. For the vacancy calculations, atoms from the 5- and 7-member rings in the grain boundary will be removed to examine the impact of each individually. The substitutional calculations will take place in the same vacant sites and involve the same impurity atoms used in the aforementioned calculations.

Conclusions can be drawn from bulk data, grain boundary data, and combined data. From the bulk vacancies, it is noted that the formation energy for the removal of C is lower than the formation energy for removing Si, indicating that C vacancies are more stable. Interstitial defects have the highest formation energy likely due to the introduction of lattice strain. Substitutional sites are the most-stable bulk defect for all impurity atoms. In fact, O and N substations into C sites are more favorable than bulk showing negative formation energies. The results for all bulk defect calculations are shown in Fig. 5.

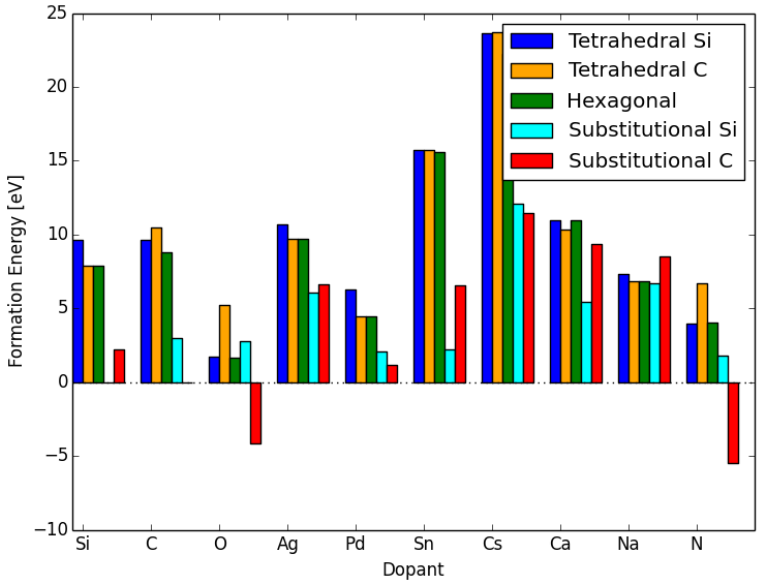

Fig. 5 Bulk formation energy for 10 impurity atoms in two substitutional sites (Si and C) and three interstitial sites (tetrahedral Si, tetrahedral C, and hexagonal)

Trends are observed from the survey of bulk defects based off characteristics of the impurity elements considered. Figure 6 shows the atomic radius for each impurity atom. By taking the ratio of the atomic radius of the impurity atom to the radius of the site it was placed, a normalized value emerges that can be used to make comparisons among all values observed. As this ratio increases, the formation energy increases for both substitutional and interstitial defects, as shown in Fig. 7. This increased in formation energy based off atomic radiuses can be correlated to the lattice strain increasing as a larger atom is placed into a site. This strain could be unfavorable, corresponding to a higher formation energy.

Fig. 6 Relative size of atomic radiuses of impurity atoms considered in this work

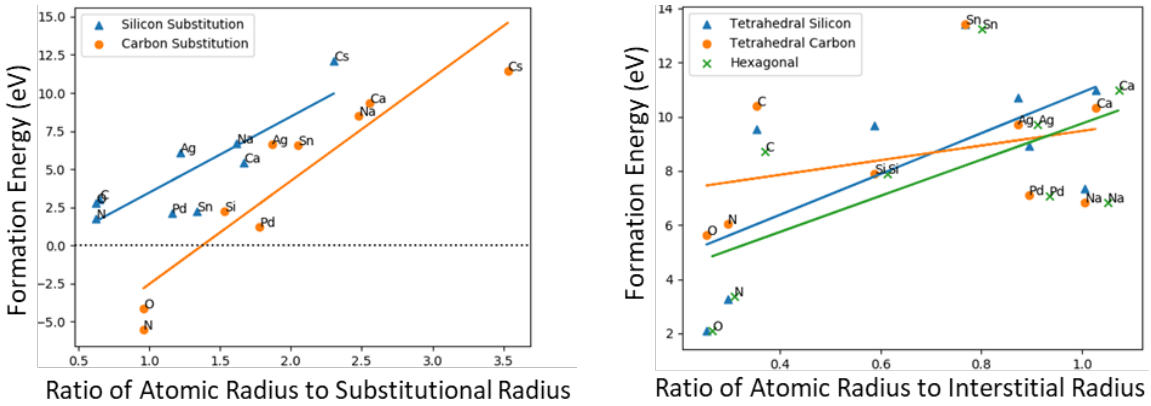

Fig. 7 Trends in formation energy for bulk SiC-3C substitutional and intestinal defects

Because the sites considered for grain boundary interstitials had larger volumes than the bulk interstitial sites, the inserted atoms were less likely to cause lattice strain. The computed formation energies show that the grain boundary interstitials are more favorable than the bulk interstitials. Some of these grain boundary interstitial values are also more favored than bulk substitutions of the same impurity atoms. However, some of these grain boundary interstitials are not lower than the bulk substitutional values, indicating that particular elements prefer to be in bulk than the grain boundary interface. This information is beneficial in knowing which atoms are likely to sit where in the SiC structure. The most-favored bulk site and grain boundary site are compared in Fig. 8.

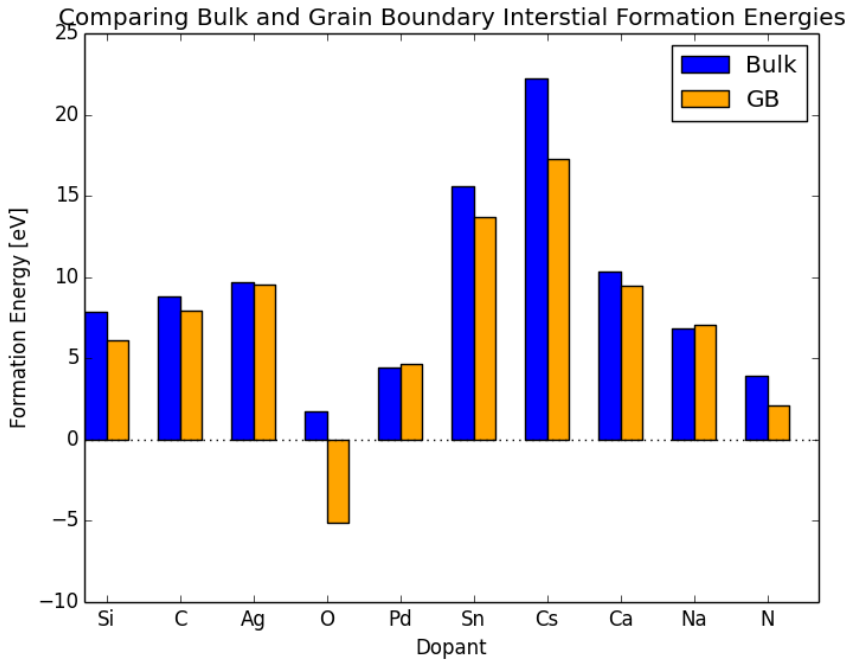

Fig. 8 Most-favored interstitial formation energies for bulk and grain boundary calculations

4. Conclusions

In this work, DFT determined the favorability of defects in the SiC system. Simulations of vacancy, substitutional, and interstitial defects were conducted in bulk SiC and symmetric tilt ∑9 {122} SiC grain boundaries. In bulk SiC, C vacancies were found to be more stable than Si vacancies, and substitutional defects were found to be more favorable than interstitial defects. The formation energy in both substitutional and interstitial sites increased as the atomic radius of the impurity atom increased. In the grain boundary, some interstitial energies were lower than the most-favored defect site in the bulk lattice, which indicates a preferential desire to segregate at the interface.

While only Σ9 {122} SiC symmetric tilt grain boundaries have been considered here, the methodology that was developed in this work can easily be expanded to other grain boundaries in SiC and for other material systems. In the future, more grain boundaries will be examined to better guide processing experiments and give deeper understanding to experimental characterization. This includes moving on to SiC–diamond composites, where the general methods developed here can be incorporated with to see how the impurities will react in more-complex heterogeneous interfaces.

5. References

1. Vargas-Gonzalez L, Speyer RF, Campbell J. Flexural strength, fracture toughness, and hardness of silicon carbide and boron carbide armor ceramics. International Journal of Applied Ceramic Technology 2010;7(5):643–651.

2. Kohyama M. Tensile strength and fracture of a tilt grain boundary in cubic SiC: a first-principles study. Philosophical Magazine Letters. 1999;79(9):659–672.

3. Rabone J, Kovács A. A DFT investigation of the interactions of Pd, Ag, Sn, and Cs with silicon carbide. International Journal of Quantum Chemistry. 2014;114(22):1534–1545.

4. The VASP manual: vaspwiki [accessed 2019 Sep 3]. https://cms.mpi.univic.ad.at/wiki /index.php/The_VASP_Manual.

5. Stukowski A. Visualization and analysis of atomistic simulation data with OVITO–the open visualization tool. Model Sim Mater Sci Eng. 2010;18:015012.

6. Momma K, Izumi F. VESTA 3 for three-dimensional visualization of crystal, volumetric and morphology data. J Appl Crystallogr. 2011;44:1272–1276.

7. Clark SJ, Segall MD, Pickard CJ, Hasnip PJ, Probert MJ, Refson K, Payne M. First principles methods using CASTEP. Zeitschrift fuer Kristallographie 2004;220(5-6):567–570.

Appendix. Example Scripts

Input Files:

INCAR

```
System = SiC
ISMEAR = 0; SIGMA = 0.1;
LREAL = AUTO
ENCUT = 500
ISYM = 2
IALGO = 48
ISTART = 0; ICHARG = 2
IBRION = 2
ISIF = 3
EDIFFG = 1.0E-06
NSW = 120
```

KPOINTS

```
Automatic mesh
0
Gamma
4 4 4
0 0 0
```

Portable Batch System (PBS) Run Script

```
#!/bin/bash
#PBS -A ARLAP38753387
#PBS -q standard
#PBS -N bulk
#PBS -l select=2:ncpus=80:mpiprocs=40
#PBS -l place=scatter:excl
#PBS -l walltime=48:00:00
#PBS -j oe
. /usr/share/Modules/init/bash

export OMP_NUM_THREADS=1
hostname
date

cd /p/home/cma14003/cassidy/bulk
pwd


mpirun                          -np                          80
/p/home/cma14003/cassidy/vasp.5.4.4/bin/vasp_std      >
vasp.out
```

```
echo "program done"
date
```

List of Symbols, Abbreviations, and Acronyms

Ag	silver
C	carbon
Ca	calcium
Cs	cesium
DFT	density functional theory
HIP-19-009	HPC Internship Program
N	nitrogen
Na	sodium
O	oxygen
PBS	portable batch system
Pd	palladium
SiC	silicon carbide
Sn	tin
VASP	Vienna Ab initio Simulation Package

1 (PDF)	DEFENSE TECHNICAL INFORMATION CTR DTIC OCA
1 (PDF)	CCDC ARL FCDD RLD CL TECH LIB
1 (PDF)	GOVT PRINTG OFC A MALHOTRA
12 (PDF)	CCDC ARL FCDD RLW MA E D WETZEL FCDD RLW ME S COLEMAN S I SIDRA J J SWAB A A DIGIOVANNI J LASALVIA M GUZIEWSKI FCDD RLW MF R J DOWDING C D HAINES K LIMMER FCDD RLW PC J CLAYTON R B LEAVY